Applied Thermal Engineering 31 (2011) 2622–2630

Contents lists available at ScienceDirect

Applied Thermal Engineering

journal homepage: www.elsevier.com/locate/apthermeng

A model of groundwater seepage and heat transfer for single-well ground source heat pump systems

Long Ni [a,*], Haorong Li [b], Yiqiang Jiang [a], Yang Yao [a], Zuiliang Ma [a]

[a] Institute of Heat Pump and Air Conditioning Technology, Harbin Institute of Technology, Harbin 150090, China
[b] Department of Architecture Engineering, University of Nebraska-Lincoln, Omaha 68182, NE, USA

ARTICLE INFO

Article history:
Received 12 July 2010
Accepted 18 April 2011
Available online 29 April 2011

Keywords:
Ground source heat pump
Single-well system
Groundwater seepage
Heat transfer

ABSTRACT

In China, for the limitation of land, many buildings intending to utilize ground source heat pump systems install "single-well" systems, which drill only one well for both the pumping and reinjection of the groundwater. A model of groundwater seepage and heat transfer for single-well ground source heat pump systems has been established and validated against the experiment conducted in Denmark. In a unitary homogenous confined aquifer, the analytic seepage solution has been derived. Moreover, equations of steady drawdown, seepage velocity, quasi-steady time and hydraulic effective radius are achieved. Results show that groundwater seepage can achieve steady state quickly. In addition, the thermal performance of groundwater and aquifer on a case study in Beijing, China has been simulated. The simulation indicates that the large thermal effective radius (far to 40 m), which is much larger than that of ground-coupled heat pump, makes one single-well accommodate large space heating and cooling loads.

1. Introduction

In recent years, ground source heat pump systems have become an important energy-saving and environmental protection technology for space heating and air-conditioning of residential and commercial buildings in China. The report on Chinese ground source heat pump pointed out that the application area of ground source heat pump had exceeded 110 million m^2 [1]. These applications included several different systems: ground-coupled heat pump (GCHP) system (usually vertical U-tube ground heat exchanger), surface water heat pump (SWHP) system (e.g. river source and seawater source) and groundwater heat pump (GWHP) system. Among these systems, the groundwater heat pump system became more popular, especially in cities full of high-density buildings in China.

The wide applications also motivate the research on groundwater heat pump. Some new systems and well configurations are put forward. One of these new systems is an alternative design commonly known as single-well ground source heat pump (SWGSHP) system which uses one well for both the drawing and returning groundwater from aquifer [2,3]. Meanwhile, in order to reduce the thermal breakthrough, there are some intervals in the well to separate the injection and production zone. This configuration is much different from the conventional double-well system, in which two wells are sufficiently separated for single pumping and reinjection. In the last decade, the SWGSHP systems had over 250 projects installed with a total construction area about 3.6 million m^2 in China [4]. Investigation of operation cost in 11 different types of buildings carried out by Beijing Municipal Bureau of Statistics shows that the space heating price of SWGSHP systems is lower than that of municipal central heating in Beijing [5].

Compared with standing column well (SCW), as shown in Fig. 1, which also utilizes groundwater drawn from and returned to the same well in a semi-open-loop arrangement, the single-well configuration has well pipe in the aquifer and the well pipe is divided into three parts by clapboards, i.e. production zone, seals zone and injection zone. While the SCW directly uses the vertical borehole to separate the well from the aquifer rather than the well pipe in the bedrock, moreover the borehole is connected from top to bottom. Therefore, most of the water flows in the borehole. However, for single-well systems, the groundwater may flow in the aquifer due to the clapboards in the well pipe. The clapboards are made by rubber and have diameter of 0.5 m as well as height of 0.35 m.

Considerable research efforts have been spent on the SCW systems in recent decades, especially on the model development and applications [6–12]. However, for single-well systems, there is a limited attention paid on model development except for a steady state mathematical model [2]. The difference of groundwater flow

* Corresponding author. Tel.: +86 451 86282123.
E-mail address: nilonggn@163.com (L. Ni).

1359-4311/$ – see front matter © 2011 Elsevier Ltd. All rights reserved.
doi:10.1016/j.applthermaleng.2011.04.030

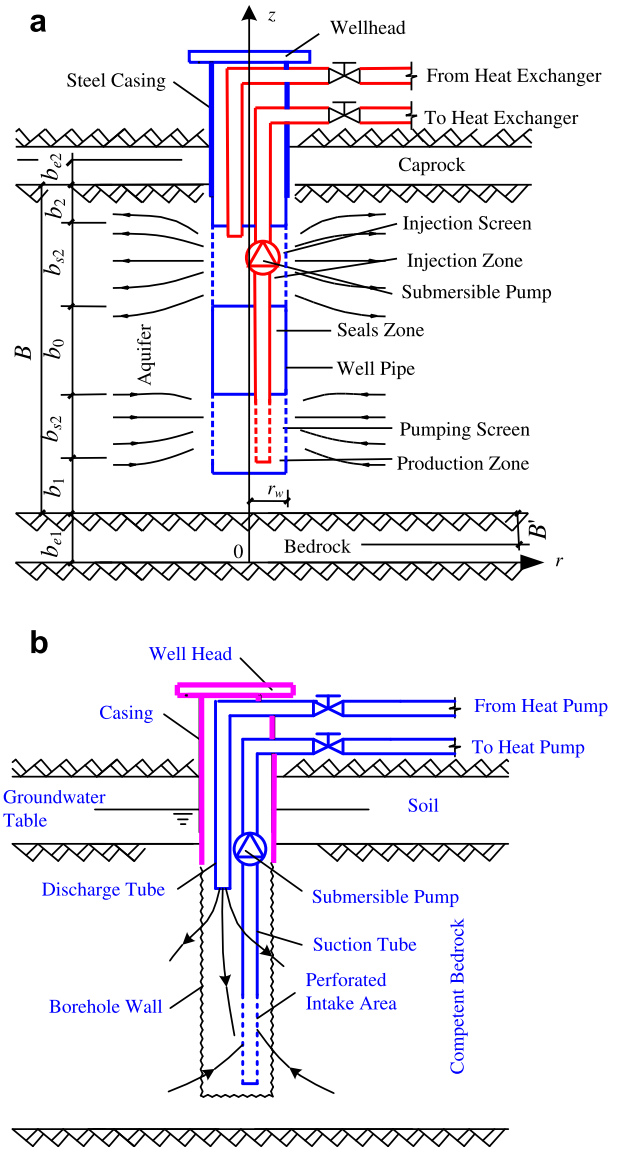

Fig. 1. A schematic diagram of single-well and SCW configuration.

between the SCW and single-well determines the big distinctions of model for groundwater seepage and heat transfer.

The goal of the research described in this paper is to develop an unsteady-state mathematical model to handle the groundwater seepage and heat transfer caused by the single-well systems. This paper first establishes a coupling model of groundwater seepage and heat transfer based on some simplified assumptions, thereafter validates the mathematical model by the field test conducted in Denmark. Moreover, the model is analyzed to achieve a theoretical solution of groundwater seepage and some discussion is spread to this theoretical equation. Finally, the model has been implemented to a case study to formulate the thermal performance of the single-well system.

2. Model development

A schematic diagram of the single-well configuration is shown in Fig. 1. In this system, the production and injection wells are integrated in one well, which is divided into three parts by clapboards: the production zone in the low part of the well, the seal zone in the middle part, and the injection zone in the top part. When the submersible pump is running, groundwater is sent to the heat exchanger at the wellhead, where it releases heat, and then is sent back to the injection space through the same well, serving as low-grade heat source and providing low-grade heat for the heat pump.

2.1. Groundwater seepage of single-well systems

2.1.1. Assumptions

The assumptions used in the groundwater seepage model are listed below

1. The aquifer is a first typical leakage confined aquifer. The non-leaky confined aquifer is regarded as a special condition of the leakage confined aquifer. Except the leakage, no vertical recharging or discharging flow is taken into account.
2. The aquifer is assumed to be homogeneous, anisotropic, horizontal, of constant thickness and of infinite lateral extent. In addition, the operation of heat pump cannot dewater the confined aquifer. When the water level falls, groundwater releases immediately from the aquifer.
3. The seepage complies with Darcy's Law.
4. The specific storativity, which is derived from the elasticity of water and aquifer matrix, is constant with time.

2.1.2. Governing equations and boundary conditions

The governing equations are presented as follows (the coordinate system is shown in Fig. 1):

$$\frac{1}{r}\frac{\partial}{\partial r}\left(K_r r\frac{\partial s}{\partial r}\right)+\frac{\partial}{\partial z}\left(K_z\frac{\partial s}{\partial z}\right)-\nu^2 s=S_0\frac{\partial s}{\partial t} \tag{1}$$

Where ν is the factor of leakage, defined as $\nu=[K_z'/(B'B)]^{1/2}$. If the cap and bedrocks are impermeable, $\nu=0$.

The initial and boundary conditions are given as:

$$\begin{cases} s|_{t=0}=0 \\ s|_{r\to\infty}=0 \\ \partial s/\partial z|_{z=0}=0 \\ \partial s/\partial z|_{z=B}=0 \\ \lim\limits_{r\to r_w} r\dfrac{\partial s}{\partial r}=\begin{cases} -\dfrac{Q_w}{2\pi K_r b_{s1}} & b_1\le z\le b_1+b_{s1} \\ \dfrac{Q_w}{2\pi K_r b_{s2}} & b_1+b_{s1}+b_0\le z\le B-b_2 \\ 0 & \text{other } z \text{ coordinates} \end{cases} \end{cases} \tag{2}$$

The seepage velocity of groundwater can be translated through drawdown, s, by adopting Darcy's Law,

$$\begin{cases} q_r=K_r\dfrac{\partial s}{\partial r} \\ q_z=K_z\dfrac{\partial s}{\partial z} \end{cases} \tag{3}$$

2.2. Heat transfer of single-well system

When the heat pump is running, the injected water with various temperatures changes the temperature of groundwater in the aquifer and the aquifer matrix, then that of the pumping water. There lie several heat transfer phenomena, which are described below. All of them but the last one (i.e. natural convection) are taken into account in the present study.

1. Thermal conduction: the injected cold or warm water exchanges heat by thermal conduction through the aquifer and its cap and bedrocks.
2. Forced convection: the forced convection is caused by the motion of the groundwater with different temperatures.
3. Thermal dispersion: the aquifer can be seen as porous media. The pulsation of velocity in the porous media pores, which results in thermal dispersion, intensifies and averages the heat transfer [13]. The heat transferred by the thermal dispersion may be very large, especially near the well [14]. The dispersion effect relates to the fluid velocity in the pores of the porous media, the properties of solid matrix and fluid as well as the structure of porous channels. Neglecting the dispersion effect may bring some inaccuracies in the simulation of the heat transfer [15].
4. Natural convection: this phenomenon, is not considered in the present study, as it is self generated by the buoyancy of the relatively warm water.

2.2.1. Assumptions

The following are some assumptions applied in the heat transfer of the groundwater and the aquifer.

1. In the heat transfer process, the temperatures of the groundwater and aquifer matrix are assumed to be identical instead of considering the water-rock thermal exchange, which has little effect on the simulation results because the duration of heat transfer between the groundwater and aquifer matrix is very short and is usually neglected [16].
2. The variation of air temperature has no effect on the groundwater temperature. The aquifer and its cap and bedrocks are in thermal equilibrium before the operation of the heat pump
3. In aquitard of the leaky aquifer, the forced thermal convection and thermal dispersion are ignored due to the low velocity of the groundwater.

2.2.2. Governing equations and boundary conditions

Considering the mass balance, energy balance and the above-mentioned assumptions, the following equation is driven:

$$C\partial T/\partial t = \mathrm{div}(k\ \mathrm{grad}\ T) - \mathrm{div}(C_w T q) \tag{4}$$

If the seepage velocity of the cap and bedrock is defined as $q_e = 0$, then the heat transfer of the aquifer and its cap and bedrocks can be unified as equation (4). Then in the aquifer and its cap and bedrocks, the parameters in equation (4) can be written as:

$$\begin{cases} T = T_{e1}, C = C_{e1}, k = k_{e1}, q = 0 & 0 \le z < b_{e1} \\ T = T_a, C = C_a, k = k_{a,ef}, q = q_a & b_{e1} \le z \le b_{e1} + B \\ T = T_{e2}, C = C_{e2}, k = k_{e2}, q = 0 & b_{e1} + B < z \le b_{e1} + B + b_{e2} \end{cases} \tag{5}$$

Translating the above equations into a columnar coordinate equation:

$$C\frac{\partial T}{\partial t} + \frac{1}{r}\frac{\partial}{\partial r}(rC_w T q_r) + \frac{\partial}{\partial z}(C_w T q_z) = \frac{1}{r}\frac{\partial}{\partial r}\left(rk_r\frac{\partial T}{\partial r}\right) + \frac{\partial}{\partial z}\left(k_z\frac{\partial T}{\partial z}\right) \tag{6}$$

The far boundary conditions and initial conditions of the aquifer and its cap as well as bedrocks can be written as follows:

$$\begin{cases} T|_{t=0} = \quad T_{r\to\infty} = T_0(z) \\ T|_{z=0} = \quad T_{e1} \\ T|_{z=b_{e1}+B+b_{e2}} = T_{e2} \end{cases} \tag{7}$$

Where the temperature $T_0(z)$ is conformed to the normal vertical temperature gradients.

However, the boundary conditions of the well are connected with the operation modes of the heat pump. The boundary conditions at $r = r_w$ are given by:

$$\begin{cases} \partial T/\partial r|_{0\le z<b_{e1}+b_1} = 0 \\ \partial T/\partial r|_{b_{e1}+b_1+b_{s1}<z<b_{e1}+b_1+b_{s1}+b_0} = 0 \\ T|_{b_{e1}+b_1+b_{s1}+b_0\le z\le b_{e1}+b_1+b_{s1}+b_0+b_{s2}} = T_p - \Delta T_h \\ \partial T/\partial r|_{b_{e1}+b_1+b_{s1}+b_0+b_{s2}<z\le b_{e1}+B+b_{e2}} = 0 \end{cases} \tag{8}$$

Where the temperature difference between the pumping and recharging water, ΔT_h, is considered positive for space heating load and negative for cooling load.

The mean pumping temperature, T_p, averaged for pumping water temperatures at different z coordinates, is shown as following

$$T_p = \int_{b_{e1}+b_1}^{b_{e1}+b_1+b_{s1}} q_r T \mathrm{d}z \Big/ \int_{b_{e1}+b_1}^{b_{e1}+b_1+b_{s1}} q_r \mathrm{d}z \tag{9}$$

2.3. Some parameters of aquifer

The specific heat capacity of the aquifer can be calculated as follows [17]:

$$C_a = nC_w + (1-n)C_m \tag{10}$$

The effective thermal conductivity of the aquifer is composed of two parts, one is the static thermal conductivity of the aquifer, while, the other is its thermal dispersion [14,18,19].

$$k_{a,ef} = k_{a,st} + \alpha C_w |q| \tag{11}$$

The static thermal conductivity of the aquifer is defined as the thermal conductivity when the groundwater does not flow. It was given as [17]:

$$k_{a,st} = nk_w + (1-n)k_m \tag{12}$$

3. Experimental validation

3.1. A brief description of the experiment

Although there are many SWGSHP systems installed in China, none of these cases has enough experimental data for the model validation. Up to now, what can be acquired is a full-scale test of the SWGSHP in the campus of Technical University of Denmark.

The single-well was 0.4 m in diameter and 45 m in depth. Two well screens were installed in the depth of 29–34 m and 38–43 m, and separated by a packer. The submarine pump was fixed at the location 2 m above the upper screen [2]. The dimensions are shown in Fig. 2.

The field test included several extraction-heat and recovery tests. For an extraction-heat test, the groundwater was pumped and extracted heat by a heat pump with the capacity of 10 kW. For a recovery test, the groundwater was reheated to the initial temperature (8.8 °C) using a 24 kW electrical heater device and was then injected to the aquifer. The volumetric flow rate of the tests was 1.5–3.0 m^3/h and the temperature difference in the extraction-heat tests was about 2–3 °C. There were 4976 m^3 of groundwater cooled and 5156 m^3 reheated [2]. The conditions of the first cycle of extraction-heat test were listed in the Table 1.

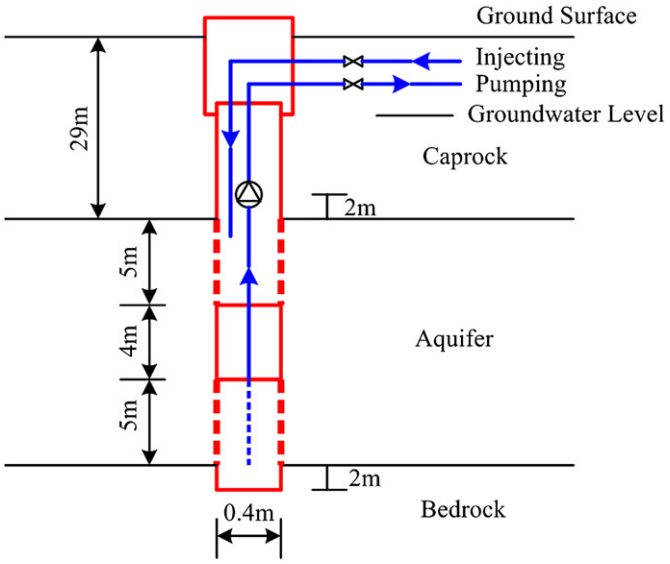

Fig. 2. The dimensions of the test single-well in the campus of Technical University of Denmark.

3.2. Model validation

The groundwater flow system of the field test could be seen as an axi-symmetric, unsteady flow in the confined aquifer. This flow and heat transfer system could be expressed by the equations in section 2.

Beside the parameters in Table 1, some other parameters, such as the heat capacity of the aquifer, the thermal dispersion length of the aquifer and thermal conductivity of the cap and bedrocks, were required for the model validation. Therefore, in order to identify these parameters, the experimental data were divided into two segments. The first 500 h' test data were selected for parameter identification and the rest for the model validation.

A sensitivity analysis of these parameters was conducted before the parameter identification. The results show that the permeability ratio of the aquifer (horizontal to vertical) and specific heat are the sensitive parameters and the thermal dispersion length of the aquifer as well as the thermal conductivity and specific heat of the cap and bedrocks have little effect on the output. As a result, the values of the thermal dispersion length, thermal conductivity and specific heat of the cap and bedrocks were preset to the model values [20]. The values of the permeability ratio and the specific heat of the aquifer were optimized through simplex search method [21].

The optimization range for permeability ratio, r_K, was 0.1–10 and for the specific heat of the aquifer, C_a, was 250–25,000 kJ/(m^3·°C). For this case, when the initial values were selected as $r_K = 0.8$ and $C_a = 2500$ kJ/(m^3·°C), the mean absolute error of the pumping groundwater temperature between the results of simulation and test was less than 0.1 °C after 27 times of iteration. The optimization values and the comparison results were presented in Table 2 and Fig. 3, respectively. As shown in the Fig. 3, the simulation values well tracked the variation of the pumping temperature except some protuberances (>0.5 °C) in the experimental data. The reason behind that might be the distortion of the temperature sensors. Meanwhile, some little fluctuations (<0.2 °C) existed in the measurement curve. These might be caused by two reasons: one is the random fluctuation of the sensors; while, the other is the small variation of the temperature difference between the pumped and injected groundwater or the little gaps between the borehole and the well pipe. Even so, the agreement between the simulation and experimental data is distinct and can be accepted.

Table 1
The conditions of the first cycle of extraction-heat test.

Contents	Unit	Values
Horizontal Permeability Coefficients of Aquifer	m/s	1.0E-4
Specific Storage	m^{-1}	1.0E-6
Thermal Conductivity of Aquifer	W/(m·°C)	3.0
Initial Temperature of Groundwater	°C	8.8
Specified Temperature Difference of Pumping and Injection Groundwater	°C	2.2
Volumetric Flow rate of Groundwater	m^3/h	1.667

Table 2
The results of parameter identification for the first cycle of extraction-heat test.

Contents	Unit	Values
Thermal Dispersion Length of Aquifer	m	1.0
Specific Heat of Caprock and Bedrock	kJ/(m^3·°C)	2500
Thermal Conductivity of Caprock and Bedrock	W/(m·°C)	2.0
Permeability Ratio (Horizontal/Vertical)	–	1.071
Specific Heat of Aquifer	kJ/(m^3·°C)	1911

4. Theoretical analyses of groundwater seepage

4.1. Analytic seepage equation

In a unitary homogenous confined aquifer, if permeability coefficients K_r, K_z and specific storativity S_0 are all constants, as shown in Fig. 4, the SWGSHP can be viewed as a combination of a partially penetrating well for pumping and a well for injection. Therefore, the groundwater seepage of SWGSHP is simply the sum of a pumping well solution and an injection well solution. Moreover, the analytic solution of a partially penetrating well for pumping has been acquired by Hantush [22]. Arranged as

$$s_1 = \frac{Q_w}{4\pi K_r B}\left\{ W(u_r, r/B_r) + \frac{2}{\pi\theta_{s1}}\sum_{n=1}^{\infty}\frac{1}{n}\left[\sin n\pi(1-\theta_1) - \sin n\pi(\theta_0+\theta_{s1}+\theta_2)\right] \times\cos\left(n\pi\theta_z'\right) W\left(u_r, \sqrt{(r/B_r)^2+(n\pi\bar{r}/B)^2}\right)\right\} \quad (13)$$

Where θ_i is defined as $\theta_1 = b_1/B$, $\theta_{s1} = b_{s1}/B$, $\theta_0 = b_0/B$, $\theta_{s2} = b_{s2}/B$, $\theta_2 = b_2/B$, $\theta_z = z/B$ and $\theta_z' = 1-\theta_z$, $W(u,x) = \int_u^\infty \exp[-y - x^2/(4y)]\,dy/y$, $u_r = r^2/(4a_r t)$, $B_r^2 = K_r/\nu^2$, $a_r = K_r/S_0$, $\bar{r} = (K_z/K_r)^{1/2} r$.

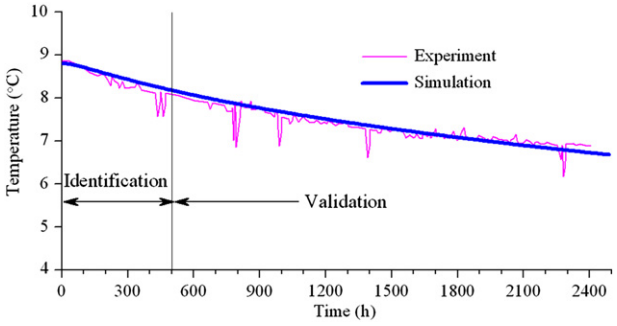

Fig. 3. Comparisons between the simulation and experimental data of the pumping temperature.

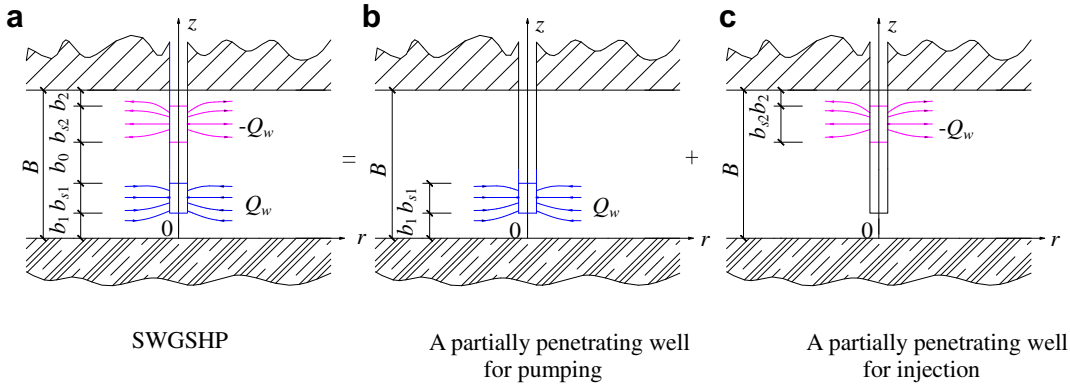

Fig. 4. A schematic drawing showing the tactic of superposition.

Define β_n and the well configuration function of pumping (WCFP), $F_p(\theta_i,n)$ as

$$\beta_n = \left[(r/B_r)^2+(n\pi\bar{r}/B)^2\right]^{1/2} \tag{14}$$

$$F_p(\theta_i,n) = \frac{2}{\pi n\theta_{s1}}[\sin n\pi(1-\theta_1)-\sin n\pi(\theta_0+\theta_{s1}+\theta_2)] \tag{15}$$

Equation (13) can be arranged as follows:

$$s_1 = \frac{Q_w}{4\pi K_r B}\left[W(u_r,\beta_0)+\sum_{n=1}^{\infty}F_p(\theta_i,n)\cos\left(n\pi\theta_z^{'}\right)W(u_r,\beta_n)\right] \tag{16}$$

The same as the solution of the well for pumping, the solution of the partially penetrating well for injection is shown as following:

$$s_2 = -\frac{Q_w}{4\pi K_r B}\left[W(u_r,\beta_0)+\sum_{n=1}^{\infty}F_r(\theta_i,n)\cos\left(n\pi\theta_z^{'}\right)W(u_r,\beta_n)\right] \tag{17}$$

Where the well configuration function of recharging (WCFR), $F_r(\theta_i,n)$, is defined as:

$$F_r(\theta_i,n) = \frac{2}{\pi n\theta_{s2}}[\sin n\pi(\theta_{s2}+\theta_2)-\sin(n\pi\theta_2)] \tag{18}$$

Thus, the drawdown of the single-well with constant flow rate in a unitary homogenous confined aquifer is $s = s_1 + s_2$, where

$$s = \frac{Q_w}{4\pi K_r B}\sum_{n=1}^{\infty}F(\theta_i,n)\cos\left(n\pi\theta_z^{'}\right)W(u_r,\beta_n) \tag{19}$$

In equation (19), the well configuration function of the sigle-well (WCFSW), $F(\theta_i,n)$, is defined as:

$$F(\theta_i,n) = F_p(\theta_i,n)-F_r(\theta_i,n) \tag{20}$$

The values of WCFSW fluctuate around zero, and tend to be zero gradually, as shown in Fig. 5. After $n = 10$, the values of WCFSW are very small and can be neglected.

4.2. Discussion

4.2.1. The steady drawdown

When time $t\to\infty$, then $u_r\to 0$, the limit of $W(u_r,\beta)$ equals to $2K_0(\beta)$. The values of $K_0(\beta)$ are approximatly equal to zero at $\beta \geq 4$. Therefore, the steady drawdown equation of the single-well in a unitary homogenous confined aquifer can be written as:

$$s_s = \frac{Q_w}{2\pi K_r B}\sum_{n=1}^{\infty}F(\theta_i,n)\cos\left(n\pi\theta_z^{'}\right)K_0(\beta_n) \tag{21}$$

The steady seepage velocities of the groundwater can be achieved by Darcy's Law using the relation, $dK_0(\beta)/d\beta = -K_1(\beta)$ [23].

$$\begin{cases} q_{r,s} = -\dfrac{Q_w}{2\pi rB}\displaystyle\sum_{n=1}^{\infty}F(\theta_i,n)\cos\left(n\pi\theta_z^{'}\right)\beta_n K_1(\beta_n) \\ q_{z,s} = \dfrac{Q_w K_z}{2K_r B^2}\displaystyle\sum_{n=1}^{\infty}nF(\theta_i,n)\sin\left(n\pi\theta_z^{'}\right)K_0(\beta_n) \end{cases} \tag{22}$$

For a specific single-well, the steady drawdown contour and velocity vectors map are shown in Fig. 6. The calculation conditions are listed in Table 3. Fig. 6 shows that the absolute values of the drawdown are very small in the middle of the aquifer due to the mixture of the pumped and injected flow. It is useful for the injection that the groundwater flows from the injuection section to the pumping section. In addition, the drawdown and seepage velocity of the groundwater varies sharply with the distance to the well axis. At location 40 m far from the well axis, the absolute value of the drawdown is less than 0.01 m.

4.2.2. The drawdown equation for long time

As mentioned above, the limit of $W(u_r,\beta)$ equals to $2K_0(\beta)$ at time $t\to\infty$. Practically, when $u<\beta^2/20$, this equation is satisfied. For equation (19), according to the definition of β_n, i.e. equation (14), the inequality $u<\beta^2/20$ is

$$u_r < \frac{1}{20}\left[\left(\frac{r}{B_r}\right)^2+\frac{K_z}{K_r}\left(\frac{n\pi r}{B}\right)^2\right] \quad n = 1,2,\ldots \tag{23}$$

Adopt $n = 1$ (If $n = 1$ is satisfied, then $n > 1$ is satisfied too), and usually $K^{'}/B^{'} << \pi^2 K_z/B$, therefore

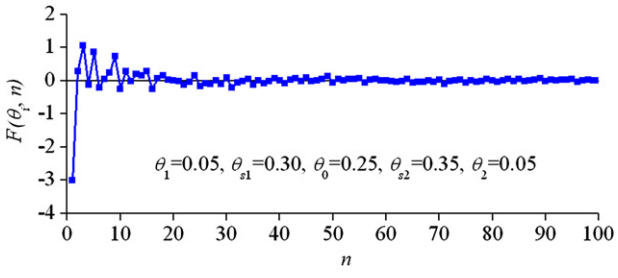

Fig. 5. The values of a certain WCFSW.

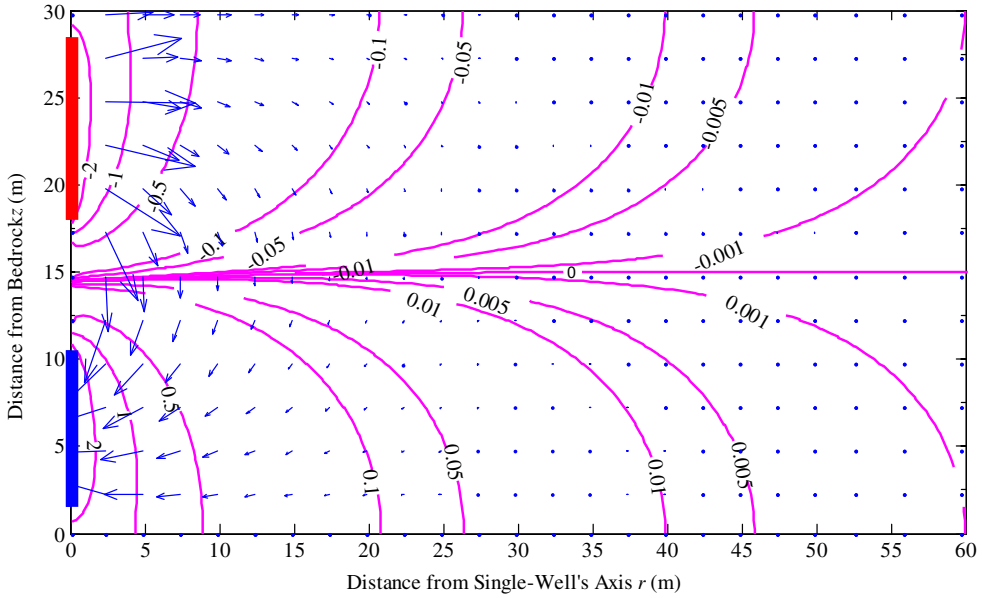

Fig. 6. Steady drawdown contour and velocity vectors map.

$$t > 5B^2S_0/\left(\pi^2K_z\right) \approx 0.5B^2S_0/K_z \tag{24}$$

When equation (24) is satisfied, equation (19) can be approximated to equation (21), that is to say, the quasi-steady state is achieved. Using t_{qs} to represent the quasi-steady state time, then

$$t_{qs} = 0.5B^2S_0/K_z \tag{25}$$

As shown in the equation (25), the time of the quasi-steady state is independent of the pumping flow rate as well as the dimensions of the well configuration. According to the conditions of Fig. 6, the quasi-steady time is only 0.6 s.

Generally speaking, if the simulation time step is 1 h or longer in a thin aquifer, the unsteady-state process of the groundwater seepage cannot be captured. The seepage process can be regarded as steady state, i.e., the equations (21) and (22) can be adopted.

4.2.3. The drawdown equation away from the single-well

The leaky well function, $W(u, \beta)$, has the property that its values decrease with the increase of β. When$\beta \to \infty$, $W(u,\beta)$=0; and when $\beta = 4$, the value of $W(u, \beta)$ is very small [24]. That is to say,

$$\sqrt{\left(\frac{r}{B_r}\right)^2 + \frac{K_z}{K_r}\left(\frac{n\pi r}{B}\right)^2} > 4 \quad n = 1, 2, \ldots \tag{26}$$

Usually, $1/B_r^2 << \pi^2K_z/(B^2K_r)$, i.e. probably when $r > 1.3B(K_r/K_z)^{1/2}$, the single-well has little effect on the groundwater flow. Using R_{th} to represent the hydraulic effective radius (HER) of the single-well, then:

$$R_{th} = 1.3B\sqrt{K_r/K_z} \tag{27}$$

Equation (27) shows that the values of R_{th} are only related to the thickness of the aquifer, B, and the ratio of the permeability coefficient (horizontal/vertical), K_r/K_z.

4.2.4. The mean drawdown in an observation well

The drawdown expressed in Equation (19) is also called piezometer drawdown, which is the drawdown of a specific spot in the aquifer. Each depth has different drawdown in the aquifer with a single-well. Thus, the drawdown in an observation well may be the mean of the drawdown in the screen of the observation well. Hantush thought that this mean value was the geometric mean of the drawdown [25]. Therefore, the mean drawdown in an observation well can be derived through the integral mean of the drawdown in the screen. Especially, the mean drawdown in a fully penetrating observation well can be derived as follows

Table 3
Calculation conditions of Fig. 6

Contents	Unit	Values
The Aquifer Thickness, B	m	30
The Distance from the Pumping Screen to the Bedrock, b_1	m	1.5
The Length of the Pumping Screen, b_{s1}	m	9.0
The Spacing between the Pumping Screen and the Recharging Screen, b_0	m	7.5
The Length of the Recharging Screen, b_{s2}	m	10.5
The Radius of the Single-Well, r_w	m	0.25
The Permeability Coefficients, K_r, K_z	m/s	7.3E-4
The Specific Storativity, S_0	m^{-1}	1.0E-6
The Groundwater Flow Rate of the Single-Well, Q_w	m^3/h	180
The Factor of Leakage, ν	$s^{-1/2}$ $m^{-1/2}$	5.8E-5

Table 4
The properties of aquifer.

Items	Unit	Values
Thickness	m	40
Horizontal Permeability Coefficient	m/s	1.0E-4
Ratio of Permeability Coefficient (Horizontal/Vertical)	–	1.0
Specific Storativity	m^{-1}	1.0E-6
Thermal Dispersion Length	m	1.0
Specific Heat Capacity	kJ/(m^3·°C)	2600
Thermal Conductivity	W/(m·°C)	2.5
Initial Temperature	°C	15

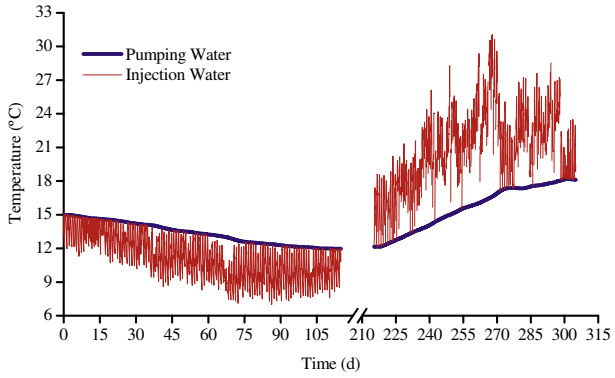

Fig. 7. Temperatures of pumping and recharging water.

$$s = \frac{Q_w}{4\pi K_r B}\sum_{n=1}^{\infty} F(\theta_i, n)\,\frac{1}{B}\,W(u_r, \beta_n)\int_0^1 \cos\left(n\pi\theta_z'\right)\mathrm{d}z = 0 \qquad (28)$$

That is to say, wherever the fully penetrating observation well is, its average drawdown is zero. Accordingly, in an aquifer with a single-well, the fully penetrating observation well might not measure any variations of the hydraulic head.

5. Thermal performance analysis

5.1. Simulation conditions

The simulation conditions were all selected from the common cases in Beijing, China. The aim aquifer is the sandy gravel aquifer with buried depth of 30 m and no leakage. The properties of the aquifer are listed in Table 4. The cap and bedrocks are both clay. Its specific heat capacity is 2600 kJ/(m^3·°C) and thermal conductivity is 1.5 W/(m·°C). The thermal conductivity of the groundwater is 0.60 W/(m·°C) and the specific heat capacity is 4176 kJ/(m^3·°C). The dimensions of the selected single-well are $r_w = 0.25$ m, $b_{s1} = 12.0$ m, $b_0 = 10.0$ m, $b_{s2} = 14.0$ m and $b_2 = 2.0$ m. The pumping and recharging flow rates of the single-well are both 40 m^3/h.

The prototype building is a typical five-floor office building with an approximate size of 5100 m^2 in Beijing, China. The hourly space heating and cooling load is provided through the building thermal simulation program DeST-c [26]. The design space heating and cooling loads are 336 kW and 575 kW, respectively. According to the distribution of the space heating and cooling loads, the heating season lasts 115 days, from November 8 to March 2 and the cooling season lasts 90 days, from June 11 to September 8. According to the space loads and the discharge of well, only one single-well can service this prototype building.

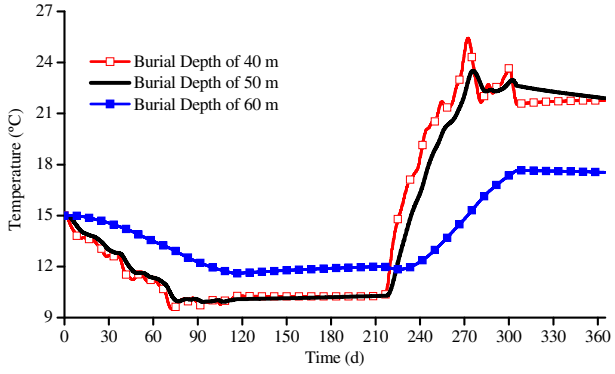

Fig. 8. Temperatures of some locations at 10 m away from well axis in the aquifer.

5.2. Results and discussion

The relationship between the temperature of the pumping and recharging water with time is shown in Fig. 7. As a whole, the temperatures of the pumping water reduce gradually with the increase of the operation time in the heating season and increase in the cooling season, which means the thermal breakthrough happens.

In the heating season, the temperature of pumping water reduces 3.04 °C. The minimum temperature of the injection water is 6.99 °C. This range of variation of the groundwater temperature has little effect on the efficiency of the heat pump unit and can be undertaken. In the beginning of the cooling season, the pumping temperature is only 12.15 °C. The temperature of the pumping water recovers to the initial temperature (15 °C) after 33 days' operation of the heat pump and reaches 18.11 °C at the end of the cooling season.

The temperatures of the aquifer also vary with the operation of the heat pump. Fig. 8 gives the temperature variations of several spots in the aquifer. Among these spots, the burial depth of 40 m is

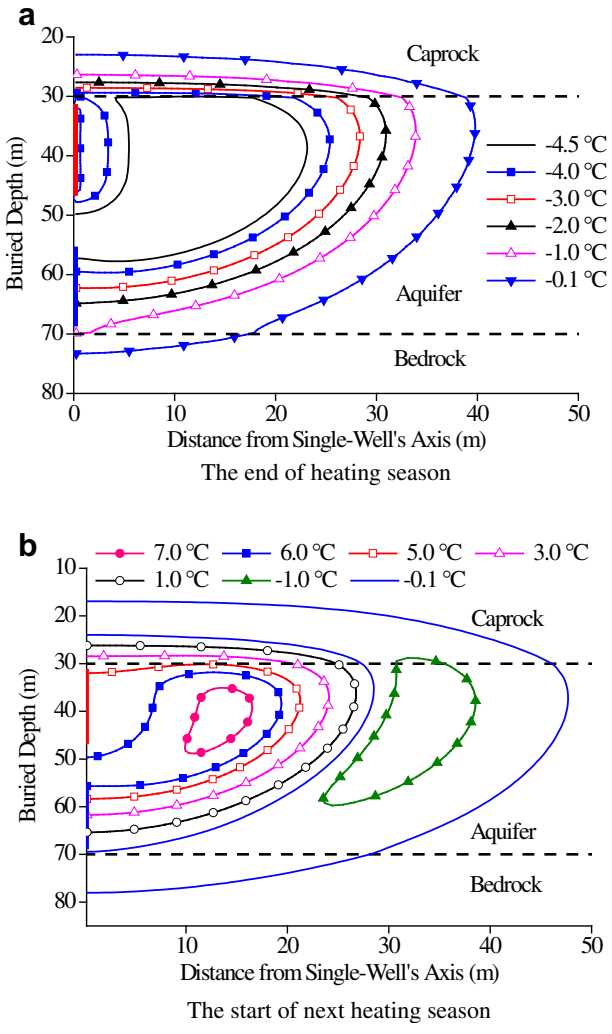

Fig. 9. Temperatures change contour of aquifer.

almost situated in the mid recharging screen, the burial depth of 50 m in the mid spacing of the pumping and recharging screen, and that of 60 m in the upper pumping screen. As shown in Fig. 8, the temperatures of the burial depth of 40 m and 50 m vary faster than that of the burial depth of 60 m. In the location of the burial depth of 40 m, the difference between the maximum and minimum temperature is as high as 15.92 °C. Therefore, attention should be paid to the thermal pollution of the groundwater and aquifer.

The contours of the temperature change in the aquifer are shown in Fig. 9. At the end of the heating season, the temperature variation is mainly located in the upper aquifer. Because of the groundwater seepage, the thermal effective radius (TER) of the single-well, which is defined as the radial distance of the aquifer with 0.1 °C temperature change, is as far as 39.8 m, which is much larger than that of the ground-coupled heat pump (usually 4–5 m). Just for the spread of TER, the pumping temperature could not change too much when the single-well accommodates large loads. As shown in Fig. 9 (b), on the beginning of the next heating season, the aquifer temperatures do not recover to the initial temperature but increase at certain locations and decrease at others. The locations of the aquifer nearer the well axis have higher temperatures. While, the temperatures of the aquifer away from the well axis are lower than the initial temperature. As a result, the quantity of accumulated heat near the well axis is much higher than the difference of the heat quantity entered into the aquifer in summer subtracting that extracted from the aquifer in winter. This storage of heat is good for the next heating season.

6. Conclusion

The utilization of shallow geothermal energy for space heating, cooling and hot water supply has aroused increasing interest in China. SWGSHP system drills only one well for both the pumping and reinjection of the groundwater, however, the installation cost can be considerably reduced. The model for groundwater seepage and heat transfer of SWGSHP systems has established and validated against experimental data in this paper. It has been demonstrated that the characteristics of the groundwater seepage and heat transfer resulted by an SWGSHP can be predicted by the model. In a unitary homogenous confined aquifer, the analytic seepage solution has been derived and the thermal response of a case study in Beijing, China has been simulated. The results show:

(1) Groundwater seepage caused by the single-well system can achieve a steady state quickly in a relative thin aquifer. The groundwater hydraulic head, some distance away from the single-well, is not influenced by the pumping and injection. The hydraulic effective radius is a function of only the aquifer thickness and ratio of permeability coefficient.
(2) For a fully penetrating observation well, the mean drawdown is zero wherever the observation well is located. Therefore, the conventional fully penetrating observation well is not suited for measuring the drawdown of the single-well system.
(3) From the heat transfer point of view, because of the convection and thermal dispersion, the thermal effective radius of the single-well groundwater heat pump system is as far as 40 m, which is much farther than that of the ground-coupled heat pump and allows one single-well to accommodate large space heating or cooling loads.
(4) The single-well systems can automatically store energy for the next heat extraction or discharge circulation due to the special well configuration. This heat storage improves the performance of the single-well system in the next space heating or cooling season.

Acknowledgement

This work was supported by the National Natural Science Foundation of China (No. 41002085) and the Ph.D. Programs Foundation of Ministry of Education of China (No. 200802131051).

Nomenclature

a_r	diffusivity of hydraulic head, m^2/s
B	thickness of the aquifer, m
B'	thickness of the aquitard, m
b_0	spacing between the pumping screen and recharging screen, m
b_1	distance from the pumping screen to bedrock, m
b_2	distance from the recharging screen to caprock, m
b_{e1}	thickness of thermostat layer in bedrock, m
b_{e2}	thickness of thermostat layer in caprock, m
b_{s1}	length of pumping screen, m
b_{s2}	length of recharging screen, m
C	specific heat capacity, $kJ/(m^3\cdot°C)$
K	permeability coefficients, m/s
k	thermal conductivity of aquifer, $W/(m\cdot°C)$
$k_{a,st}$	static thermal conductivity of aquifer, $W/(m\cdot°C)$
$k_{a,ef}$	effective thermal conductivity of aquifer, $W/(m\cdot°C)$
K_z'	vertical permeability coefficient of aquitard, m/s
n	porosity of aquifer, %
q	seepage velocity of groundwater, m/s
Q_w	groundwater flow rate, m^3/s
r	radial coordinate, m
$\bar{r}$	relative radial coordinate, m
r_K	permeability ratio of aquifer (horizontal to vertical)
R_{th}	hydraulic effective radius, m
r_w	radius of single-well, m
s	groundwater drawdown, mH_2O
s_1	groundwater drawdown of pumping well, mH_2O
s_2	groundwater drawdown of injection well, mH_2O
s_s	steady groundwater drawdown, mH_2O
S_0	specific storativity, m^{-1}
t	coordinate of time, s
t_{qs}	quasi-steady state time, s
T	temperature, °C
T_0	initial temperature, °C
T_p	pumping temperature, °C
z	vertical coordinate, m
α	thermal dispersion length, m
ν	factor of leakage, $s^{-1/2}\ m^{-1/2}$
ΔT_h	temperature difference of the production and injection water, °C
$F_p(\theta_i,n)$	the well configuration function of pumping
$F_r(\theta_i,n)$	the well configuration function of recharging
$F(\theta_i,n)$	the well configuration function of single-well
$K_0(\beta)$	modified Bessel function of the second kind for order zero
$K_1(\beta)$	modified Bessel function of the second kind of order one
$W(u_n, \beta_n)$	first type leaky well function with constant groundwater flow

Subscripts

‘	aquitard
a	aquifer
$e1$	bedrock
$e2$	caprock
ef	effective
m	aquifer matrix
p	pumping water
qs	quasi-steady state

r	axial coordinates
s	steady state
st	static
w	groundwater
z	vertical coordinates

References

[1] W. Xu, Repot on China Ground-Source Heat Pump. China Architecture & Building Press, Beijng, 2008, (in Chinese).
[2] S.N. Sorensen, J. Reffstrup, Prediction of Long-Term Operational conditions for single-well groundwater heat pump Plants, In: Proceedings of the 27th Intersociety Energy Conversion Engineering Conference, vol. 4, San Diego, CA, USA, 1992, pp. 4.109–104.114.
[3] S. Xu, L. Rybach, Utilization of shallow resources performance of direct use system in Beijng, Geotherm. Resour. Council Trans. 27 (2003) 115–118.
[4] Z. Yang, M. Qu, Applications and development of single-well technology in China, J. HVAC 36 (2006) 208–210 (in Chinese).
[5] L. Ni, Y. Jiang, Y. Yao, Z. Ma, Groundwater heat pump with pumping & recharging in the same well in China, In: M. Liu, J. Zhang (eds.), Sixth International Conference for Enhanced Building Operations, vol. 3, Allied Kingsway Publishing International, Shenzhen, China, 2006, pp. VIII-10–14.
[6] Z. Deng, S.J. Rees, J.D. Spitler, A model for annual simulation of standing column well ground heat exchangers, HVAC Res. 11 (2005) 637–655.
[7] Z.D. O'Neill, J.D. Spitler, S.J. Rees, Modeling of standing column wells in ground source heat pump Systems, In: Proceedings of the tenth International Conference on Thermal Energy Storage - ECOSTOCK, New Jersey, 2006, pp. (CD-ROM).
[8] Z.D. O'Neill, J.D. Spitler, S.J. Rees, Performance analysis of standing column well ground heat exchanger systems, ASHRAE Trans. 112 (2006) 633–643.
[9] C.D. Orio, Geothermal heat pump applications industrial/commercial, Energy Eng. 96 (1999) 58–79.
[10] C.D. Orio, Geothermal heat pumps and standing column wells, Geotherm. Resour. Council Trans. 18 (1994) 375–379.
[11] C.D. Orio, C.N. Johnson, K.D. Poor, Geothermal standing column wells: ten years in a New England School, ASHRAE Trans. 112 (2006) 57–64.
[12] C.D. Orio, C.N. Johnson, S.J. Rees, S. Body, A survey of standing column well installations in North America, ASHRAE Trans. 111 (2005) 109–121.
[13] M. Deleglise, P. Simacek, C. Binetruy, S. Advani, Determination of the thermal dispersion coefficient during radial filling of a porous medium, J. Heat Trans. 125 (2003) 875–880.
[14] Y. Xue, C. Xie, Q. Li, Aquifer thermal energy storage: a numerical simulation of field experiments in China, Water Resour. Res. 26 (1990) 2365–2375.
[15] B. Alazmi, K. Vafai, Analysis of variable porosity, thermal dispersion, and local thermal nonequilibrium on free surface flows through porous media, J. Heat Trans. 126 (2004) 389–399.
[16] Y. Benderitter, B. Roy, A. Tabbagh, Flow characterization through heat transfer evidence in a carbonate fractured medium: first approach, Water Resour. Res. 29 (1993) 3741–3747.
[17] W.C. Walton, Practical Aspects of Groundwater Modeling-Flow, Mass and Heat Transport and Subsidence and Computer Models, second ed. McGraw-Hill Book Company, New Jersey, USA, 1985.
[18] S. Chevalier, O. Banton, Modeling of heat transfer with the random walk method. Part 1. Application to thermal energy storage in porous Aquifers, J. Hydrol. 222 (1999) 129–139.
[19] J.P. Sauty, A.C. Gringarten, A. Menjoz, S. Body, Sensible energy storage in aquifers 1. Theoretical study, Water Resour. Res. 18 (1982) 245–252.
[20] J.P. Sauty, A.C. Gringarten, H. Fabri, S. Body, Sensible energy storage in aquifers 2. Field experiments and comparison with theoretical results, Water Resour. Res. 18 (1982) 253–265.
[21] T.H. Cormen, C.E. Leiserson, R.L. Rivest, C. Stein, Introduction to Algorithms, second ed. MIT Press and McGraw-Hill, 2001.
[22] M.S. Hantush, Drawdown around a partially penetrating well, J. Hydraul. Div. 87 (1961) 83–98.
[23] S.S. Bayin, Essentials of Mathematical Methods in Science and Engineering. John Wiley & Sons, Inc., 2008.
[24] F.W. Schwartz, H. Zhang, Fundamentals of Ground Water. John Wiley & Sons, Inc., 2003.
[25] M.S. Hantush, Aquifer test on partially penetrating wells, J. Hydraul. Div. 87 (1961) 171–195.
[26] DeST Development Group in Tsinghua University, Building Environmental System Simulation and Analysis-DeST (in Chinese). China Architecture & Building Press, Beijing, 2006.